COMPTON SCATTER PARTIAL LINE IMAGING FOR NON-INTRUSIVE INSPECTION OF LAYERED OBJECTS

Balza Achmad *)

ABSTRACT

Imaging in general can be carried out in three fashions, point-by-point, line-by-line, and plane-by-plane. In inspecting layered object, however, line imaging along the thickness of the inspected object is more preferable. Furthermore, if the region-of-interest inside the object is known in advance, partial imaging is beneficial since it does not require scanning of the whole object. This paper combines the two techniques, hence called as partial line imaging, using Compton scattering. The method is useful for instance in detecting sheet explosives concealed inside passenger's baggage as well as inspecting adhesively bonded metals or composites.

INTRODUCTION

Nuclear methods have been utilized in non-destructive testing for years, as the alternatives of many other techniques, such as those employing penetrating liquids, eddy currents, magnetic fields, microwaves, and ultrasounds. These methods include the use of radiation particles such as neutron, photon, proton, gamma, and X-rays (Alexander, et al., 1996). Nuclear radiations, however, are the best candidates especially for subsurface imaging (Achmad, 2000), while other types of sources have disadvantages for this purpose (Bray, 1992). There are three modalities in the use of nuclear radiations for non-destructive evaluations: transmission, emission, and scattering. For the reasons explained by Hussein (1990), transmission radiation as used in CT-Scan not only has several inherent limitations but also involves a very complex reconstruction process. Emission radiation is not also suitable for many applications since it usually needs source generator such as cyclotron nearby (Achmad, 2001). Compton scattering modality is therefore suitable for non-intrusive inspection since it has the ability to do point-by-point sampling hence does not require complex reconstruction process in producing images.

Some applications do not necessitate the whole inspected object to be imaged, especially if the region-of-interest is known in advance. For example, the part that suffered friction the most is a potential location of defects inside many mechanical equipment. Another case is when there is a suspect that bonding adhesive creates voids between layered metals or composites. In this case, it is preferable to do partial imaging

*) Instrumentation Laboratory and Computation Laboratory, Department of Engineering Physics, Gadjah Mada University.

that will be done only on the suspected location. Many works have been done in developing region-of-interest or partial imaging (Tonner et al, 1989; Gentle and Spyrou, 1990; Achmad, 2001).

In inspecting layered objects non-intrusively, complete imaging is surely inappropriate since the information needed usually concerns with the variations along its thickness. Conventional radiography is also not suited for this purpose since the image produced represents the integral along the path the radiation passes the object. Compton imaging, on the other hand, might be used. Jama et al (1998), used gamma ray Compton scattering to detect debonding in composite-aluminum joints by unfolding measured spectrum gathered by radiation detection system. This technique in fact was not really an imaging system, since it produced indication spectrum that needs to be analyzed further to detect the debondings. If the aim is to obtain quantitative information about the layers composing the object, then another technique has to be developed.

THE TECHNIQUE

In this research, a technique is developed by employing photon radiations emitted from radioisotopes that go through the thickness of an object. As it passes the object, some of the photons with specific energy (E) undergo collisions with free electrons inside the object that change their energies (E') and directions (θ). If the scattered photons go toward a collimated detector, then it produces electrical pulses that in turn are counted by the detection system. The detector response, i.e. the ratio between detector count and the activity of the radiation source at certain energy and scattering angle (S) can be formulated as (Hussein, 1990):

$$S(E,\theta) = k(E,\theta) f_i \rho_v^e f_s \qquad (1)$$

where $k(E,\theta)$ is a system constant, f_i and f_s are the incident and scattering attenuation factors, and ρ_v^e is the electron density at specific location (voxel, volume element) inside the object.

The system constant k is material independent and thus can be determined in advance by means of calibration or calculation. The attenuation factors, however, depend on the electron densities along the incident path and scattering path respectively, which are unknown. Hussein et al (1986) considered the attenuation problem as a non-linear problem in the imaging of a section and solved the electron densities of the entire section at once. However, the approach is not applicable for partial imaging.

In this research, the incident attenuation factor preceding the first voxel and the scattering attenuation factors toward the detectors can be cancelled out by the use of two detectors and two photon energies (**Figure 1**). The electron density of certain voxel along the imaged line therefore can be solved using the detector responses gathered from the measurements and the electron densities of the preceding voxels. A matrix equation can then be constructed to solve the electron densities of the voxels.

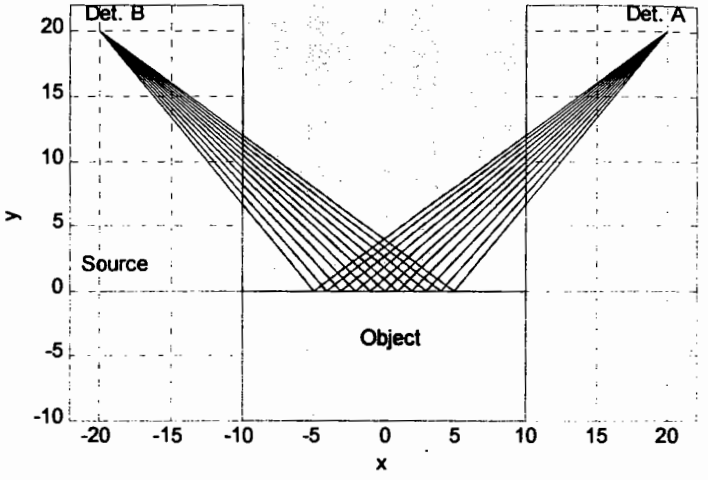

Figure 1. Source-Detectors Configuration

$$[M]\ \{\ln(\rho^e)\} = \{\ln(S)\} - \{\ln(K)\} + \{f(\rho^e)\} \quad (2)$$

where $[M]$ is a matrix composed of Compton cross-sections function of photon energy and scattering angle; $\{ln(\rho^e)\}$ is a vector containing the logarithm of the unknown electron densities; $\{ln(S)\}$ and $\{ln(K)\}$ are vectors composed of the logarithm of detector responses and system constants, respectively; and f is the attenuation factors inside the voxels. The electron densities (ρ^e) can be solved by inverting the equation.

$$\{ln(\rho^e)\} = ([M]^T[M])^{-1}[M]^T(\{ln(S)\} - \{ln(K)\} + \{f(\rho^e)\}) \quad (3)$$

However, since ρ^e also appears at the right hand side of the above equation, the solution can then be obtained by means of iteration. Firstly, a guessed value, the electron density of water, is set for ρ^e. Then ρ^e is updated using Eq. (3). The procedure is repeated until some convergence criteria achieved. The obtained electron densities of the voxel are normalized to that of water. This normalization also helps in reducing the condition number of the inverted matrix (Achmad, 2000).

The detector responses are analyzed using photon energy discriminators such as multichannel analyzer (MCA) in addition to hard collimation using highly absorbing material such as lead. The levels of discrimination are set based on the unique relationship between scattering angle and energy.

EXPERIMENTAL SETUP

The experiment was done using source-detectors configuration illustrated in **Figure 1**. Since the technique needs two distinct photon energies, two different radioisotopes were used, Cs-137 with photon energy of 662 keV and Hg-203 with photon energy of 279 keV. Those radioisotopes have been used for many applications and suited for Compton scatter imaging (Hussein, 1990). The sources were positioned 10 cm apart from the object and collimated such that photons were emitted to a specific direction

across the object. The direction of the photon beam dictated the region-of-interest and hence the line being imaged.

Two spectroscopic detectors, Detector A and Detector B, were placed at the back and the front of the object at scattering angle around 45° and 135°. In this research, NaI(Tl) detectors were used coupled with a computer-based MCA to enable simultaneous measurements using multiple detectors. The region-of-interest was a 10 cm line across the center of the object, which was actually the intersection between source photon beam and detectors' field-of-views.

The object itself was varied for different cases. In the first case, a 20 cm thick lucite block was used for the inspected object. Four measurements, two measurements for each detector, were performed using the two sources. The detector responses were then put into Eq. (3) and the electron densities along the imaged line were calculated. Afterward, the results were compared to the actual or theoretical values to determine the performance of the developed technique. The object was then varied to simulate layered object, using lucite-wood, wood-lucite, and two lucite blocks separated by void. The later was to simulate an absence of any layer inside the object or a presence of debonding.

RESULTS AND DISCUSSION

Detector Responses

The detector responses were calculated by taking the ratio between detector counts and source activities, therefore they could be compared to the theoretical value calculated using mathematical models described by Eq. (1). **Figure 2** shows the comparison between theoretical and experimental detector responses for all cases. It can be seen that the measured responses agreed with the modeled values.

The relative errors i.e. the relative difference between measured and theoretical detector responses spanned from –19.6% up to 16.7% with an average value of –0.9%. Higher relative errors were found mostly at the voxels that were farther from the source (Detector B, voxel 6 up to 10) because the detector responses at these voxels were lower than those of the others. The relative errors were also higher at the interfaces between materials, i.e. interface between lucite and wood (**Figure 2**b and c) as well as lucite and void (**Figure 2**d). The actual voxel shape was not a cube but an intersection between two cones, i.e. photon beam and detector field-of-view; therefore, some of the neighboring materials were included within a voxel located at the interface.

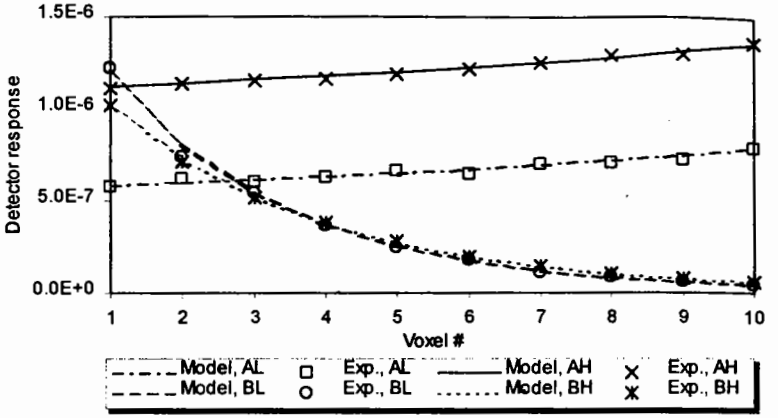

(a) lucite block

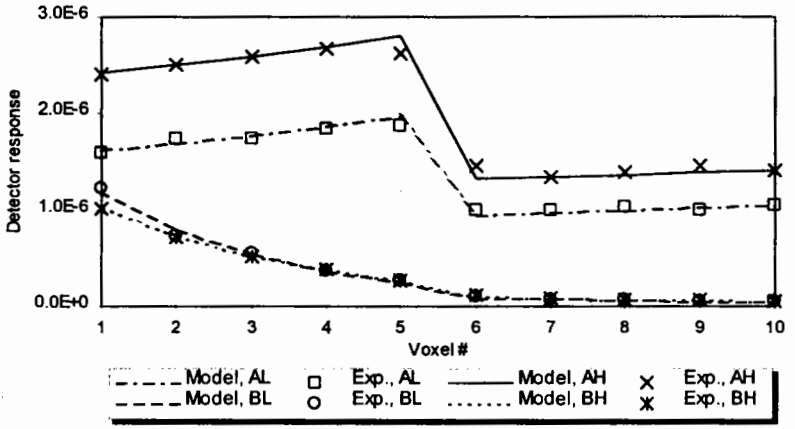

(b) lucite-wood

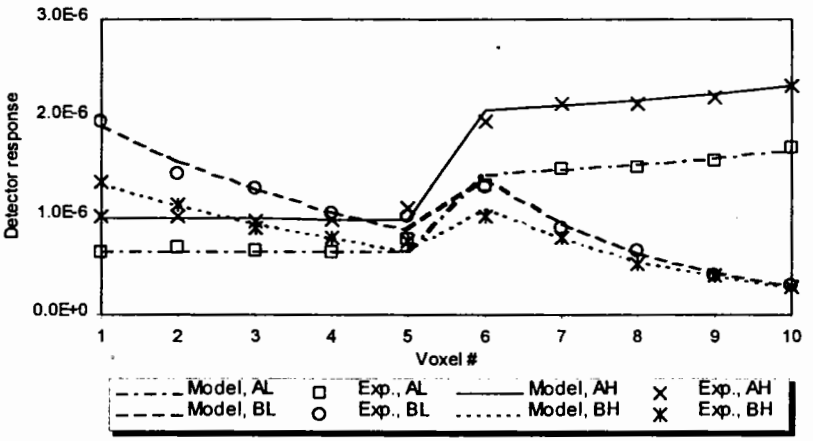

(c) wood-lucite

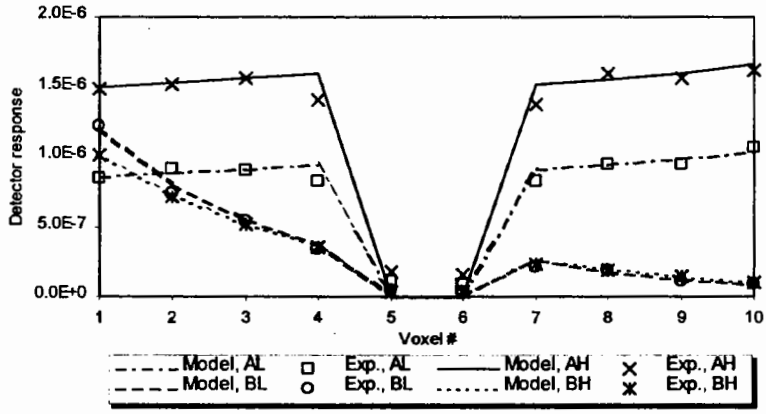

(d) two lucite blocks separated by void

Figure 2. Theoretical and Measured Detector Responses

Electron Densities of the Imaged Line

Using Eq. (3), the electron densities of the voxels were evaluated and the results were presented in Figure 3. For all cases, the calculated electron densities were close to the corresponding hypothetical values. The relative errors of the electron densities laid between -20.6% up to 17.7% with an average value of 0.3%. These errors were similar to the errors of detector responses. Higher errors in electron densities, again, occurred at the voxels that were located far from the source where their detector responses were low as well as at the interfaces between two materials (voxel 5 and 6 of Figure 3b and d). Other voxels, however, had a very good agreement with the actual values.

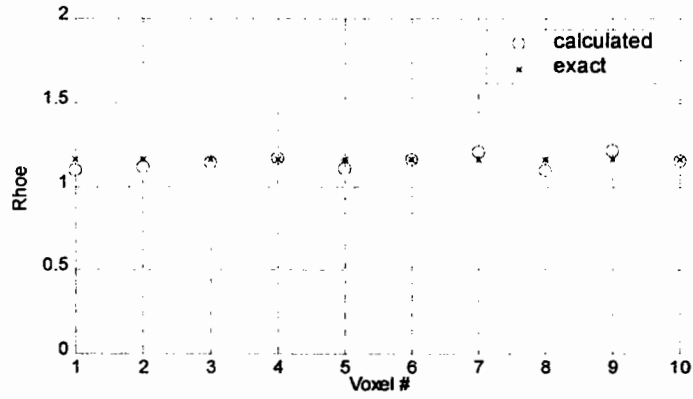

(a) lucite block

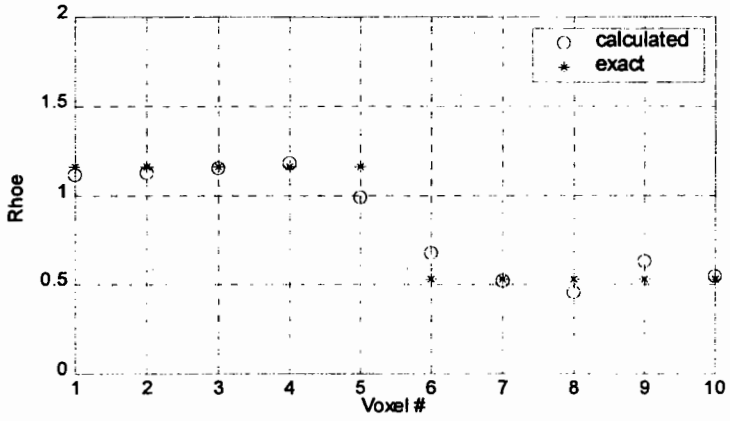

(b) lucite-wood

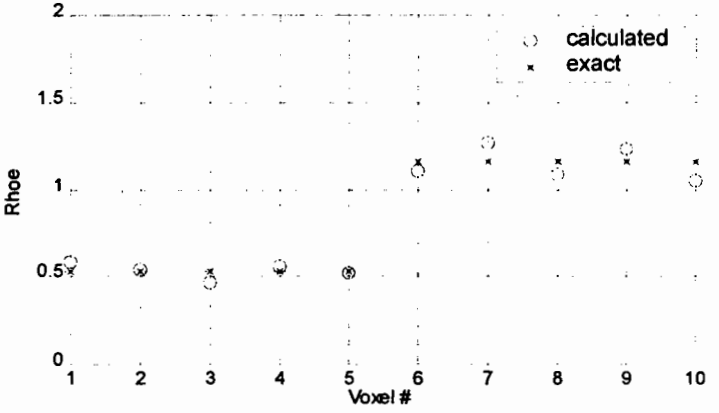

(c) wood-lucite

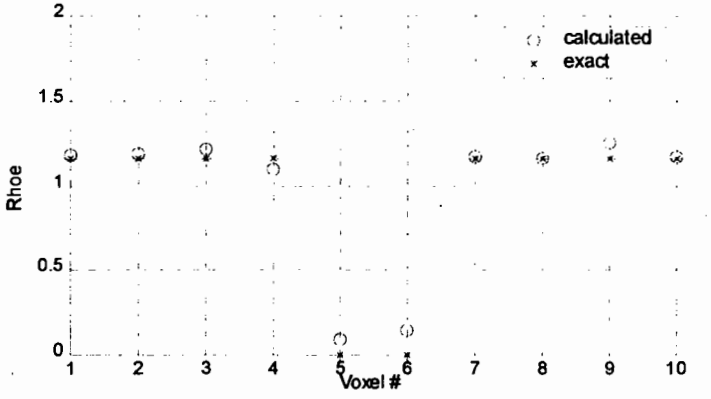

(d) two lucite blocks separated by void

Figure 3. Theoretical and Measured Electron Densities

Electron density is a function of mass density. Therefore, it can be used to investigate the internal condition of the object, i.e. the presence of defects inside the object as well as the thickness of layered materials. To enable imaging, one must incorporate scanning mechanism that facilitates measurements of a volume within the inspected object. The obtained electron density can then be displayed using visualization software.

Although there were some errors take place at some cases, the method was generally success in calculating the electron densities of a line within the inspected objects. Those errors can be minimized by increasing the fluence of the photon beam, i.e. by increasing the intensity of the sources and/or increasing the measurement time. Nevertheless, some work must be performed in order to optimize the photon fluence since increasing it will consequently increase hazard dose to the operator and the environment as well as increase the operating cost. Other effort can be made to substitute the radioisotope sources by x-rays, hence the intensity can be adjusted easily.

CONCLUSION

It has been demonstrated that the proposed method worked well when used to non-intrusively image layered objects. The measured electron densities had some errors relative to the hypothetical values. This was mostly due to the low detector responses gathered from the corresponding voxels, which were susceptible to high statistical error. This problem, however, can be resolved by increasing the fluence of the photon beam from the sources.

ACKNOWLEDGEMENT

The author thanks Dr. Esam M.A. Hussein of the X-Ray Laboratory and Laboratory for Thread Material Detection (LTMD), Department of Mechanical Engineering, the University of New Brunswick, Canada, for the facilities and computer codes used for this research.

REFERENCES

Achmad, B., 2001, Point-by-Point Partial Imaging for Non-Destructive Evaluation using Radiation Scattering Technique, in *Forum Teknik*, Vol. 25, No. 1.

Achmad, B., 2000, *X-Ray Compton Scatter Density Measurement at a Point within an Object*, M.Sc.E. Thesis (unpublished), Mechanical Engineering Department, University of New Brunswick, Fredericton.

Alexander, W.O., Davies, G.J., Heslop, S., Reynolds, K.A., and Whittaker, V.N., 1996, *Dasar Metalurgi Untuk Rekayasawan*, PT. Gramedia Pustaka Utama, Jakarta.

Bray, D.E., and McBride, D., 1992, *Nondestructive Testing Techniques*, Willey-interscience Publication, New York.

Gentle, D.J., and Spyrou, N.M., 1990, Region of Interest Tomography in Industrial Applications, in *Nuclear Instruments and Methods in Physics Research*, A299, pp 534-537.

Hussein, E.M.A., 1990, Compton Scatter Imaging Systems, in Wise, D.L. (ed.), *Bioinstrumentation: Research, Development, and Applications*, Chapter 35, pp. 1053-1086, Butterworths Publ., Storeham.

Hussein, E.M.A., Meneley, D.A., 1986, On the Solution of the Inverse Problem of Radiation Scattering Imaging, in *Nuclear Science and Engineering*, No. 92, pp. 341-349.

Jama, H.A., Hussein, E.M.A., Lee-Sullivan, P., 1998, Detection of Debonding Composite-Aluminum Joints using Gamma-Ray Compton Scattering, in *NDT&E International*, Vol. 31, No. 2, pp. 99-103.

Tonner, P.D., Sawicka, B.D., Tosello G., and Romaniszyn, T., 1989, Region-of-Interest Tomography Imaging for Product and Material Characterization, in *Proc. of the Industrial Computerized Tomography*, American Society for Nondestructive Testing, July 25-27 1989, Seattle, pp. 160-165.